

Noise thresholds for optical quantum computers

Christopher M. Dawson,¹ Henry L. Haselgrove,^{1,2} and Michael A. Nielsen¹

¹*School of Physical Sciences, The University of Queensland, Queensland 4072, Australia*

²*Information Sciences Laboratory, Defence Science and Technology Organisation, Edinburgh 5111 Australia*

(Dated: November 1, 2018)

In this paper we numerically investigate the fault-tolerant threshold for optical cluster-state quantum computing. We allow both photon loss noise and depolarizing noise (as a general proxy for all local noise), and obtain a *threshold region* of allowed pairs of values for the two types of noise. Roughly speaking, our results show that scalable optical quantum computing is possible for photon loss probabilities $< 3 \times 10^{-3}$, and for depolarization probabilities $< 10^{-4}$.

PACS numbers: 03.67.-a, 03.67.Lx

Optical systems are promising candidates for quantum computation, due to their long decoherence times, accurate single-qubit gates, and relatively efficient readout. A scheme for optical quantum computing has been suggested by Knill, Laflamme and Milburn (KLM) [1], and the basic elements of that scheme experimentally demonstrated [2, 3, 4, 5]. Unfortunately, KLM requires tens of thousands of optical elements to achieve a *single* entangling gate operating with high probability. A recent proposal [6] (c.f. [7]) combines elements of KLM with the cluster-state model of quantum computation [8] to reduce the complexity by many orders of magnitude. This scheme has been simplified [9] to require only tens of optical elements per logical gate. A recent experiment [10] demonstrated simple optical cluster state computing.

Our paper investigates the effect of noise on the optical cluster state proposals. In the standard quantum circuit model, the noise threshold theorem shows that provided the amount of noise per elementary operation is below the threshold, scalable quantum computation is possible. Unfortunately, this result does not apply directly to optical cluster states, as the cluster state model is fundamentally different from the circuit model. However, [11, 12] (c.f. [13]) established the *existence* of a threshold for clusters, without obtaining a value, while [14] argued that in a certain noise model the cluster threshold is no more than an order of magnitude worse than the circuit threshold. This latter work is not directly relevant to optical clusters, since it uses deterministic entangling gates, and does not include any process analogous to photon loss.

We use numerical simulations to find the noise threshold. Our analysis is tailored to the dominant sources of noise in optical quantum computing, including the non-determinism of the optical entangling gates, photon loss, and depolarizing noise. We therefore obtain a *threshold region* of noise parameters for which scalable optical quantum computing is possible. Our protocol is complex, and we omit some details; full details will appear in [15].

A prior work [16] has calculated a threshold for optical quantum computation when the only source of noise is photon loss. In real experiments other noise sources such as dephasing are also present, and protocols such as [16] will actually amplify the effects of such noise at the en-

coded level. By contrast, our protocol protects against both photon loss and depolarizing noise, and by standard fault-tolerance results thus automatically protects against arbitrary local noise, including dephasing (in any basis), amplitude damping, etc.

Introductions to cluster-state computation may be found in [17, 18], and we assume familiarity with the model. An important element in the model are the Pauli “byproduct” operators, known functions of the measurement results, which are used to correct the state when the computation concludes. We call the tensor product of these byproduct operators the *Pauli frame*, and it is updated after measurements of cluster qubits according to a set of *propagation rules*, described, e.g., in [17].

Our approach to optical cluster-state computation is based most closely on [9]. We use the polarization of a single photon to encode a single qubit, and build clusters up using *fusion gates* (“type I fusion gates” in [9]), which, when applied to two cluster qubits either (a) fuse the qubits into a single cluster qubit, which occurs with probability $\frac{1}{2}$; or (b) measure both qubits in the computational basis, also with probability $\frac{1}{2}$.

Available physical resources and noise: Our resources are: (1) a source of polarization entangled Bell pairs; (2) single-qubit gates, effected using linear optics, as in KLM; (3) efficient polarization-discriminating photon counters capable of distinguishing 0, 1 and 2 photons; (4) fusion gates, built from beamsplitters and photon counters; and (5) quantum memory gates. We assume all these elements take the same amount of time, and describe our circuit as a sequence of such time steps.

Our noise model includes a parameter γ representing the probability per qubit per time step of photon loss. We assume this probability is independent of the state of the qubit, and that photon loss occurs after Bell-state preparation, and before memory, single-qubit and fusion gates; for two-qubit operations we assume photon loss occurs independently for both qubits. Our noise model also includes a *depolarizing parameter* ϵ . Depolarizing noise affects physical operations as follows: (1) after Bell-state preparation or before a fusion gate the two qubits are collectively depolarized, i.e., with probability $1 - \epsilon$ nothing happens, while with probabilities $\epsilon/15$ we apply

each of the 15 non-identity Pauli operators IX, XX etc; and (2) before memory, single-qubit and measurement gates the qubit is depolarized with parameter ϵ .

Additional noise sources that may effect real implementations include dark counts and dephasing. However, the fault-tolerant protocol we implement automatically protects against such noise sources, and we believe the threshold results will not qualitatively change.

Method of simulation: We use the stabilizer formalism to simulate Clifford group operations, which are sufficient to simulate error-correction and depolarization. In our simulations, rather than working with the state directly, we merely keep track of the *errors* in the state when compared with an ideal reference state. We keep track of two types of errors: the physical error in the state of the cluster, which is represented as a tensor product of Pauli operators, and errors in the Pauli frame due to erroneous measurement results, which are again a tensor product of Pauli operators. Note that physical errors may propagate to become Pauli frame errors when qubits with physical noise are measured, giving rise to incorrect measurement results. The rules for propagating both types of errors may be computed following, e.g., [17]; see [15].

These methods suffice to describe error-correction and Pauli-type noise, but not photon loss and fusion gate failures. We can use postselection and repetition to effectively eliminate photon loss and fusion gate failures, whenever those failures do not directly affect the encoded data. However, when they do affect the data, another approach must be taken. Suppose when fusion gate failure occurs the experimenter: (1) Randomizes the local Pauli frame of the data qubit; (2) notes the location at which the failure occurred, for use in decoding; and (3) carries out the rules for propagating the Pauli frame, as though the fusion gate had succeeded, and the bond was created. The rules for propagating Pauli frame errors can be used to show that once the experimenter has randomized the Pauli frame, it does not make any physical difference whether the fusion gate failed or not, and so we can treat it as though it succeeded. The remaining errors are Pauli-type errors, and so can be simulated in the standard way. The details (and a discussion of photon loss, which is dealt with similarly) appear in [15].

Broad picture of fault-tolerant protocol: The protocol is split into two parts: (1) a cluster-based simulation of a variant of Steane’s protocol [19]; (2) a deterministic gate-based protocol, again based on [19]. The cluster threshold is obtained by concatenating the results from a single level of the cluster protocol with multiple levels of the deterministic protocol. The idea is to take a quantum circuit, build up a fault-tolerant simulation through multiple levels of concatenation in the circuit model, and then replace the bottom level by a clusterized simulation of a noisy deterministic gate.

Microclusters and parallel fusion: Our protocol is based on *microclusters*, star-shaped clusters with a central *root node*, and attached *leaf nodes*. Such microclusters can be created using repeated fusion of Bell pairs. By

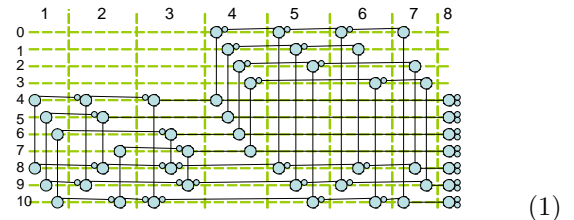
attempting preparation of a large number of microclusters in parallel and postselecting on successful attempts we can build a k -leaf microcluster in $O(\log(k))$ timesteps, and consuming $O(k^2)$ Bell pairs, with probability of success arbitrarily close to one.

Microclusters can be used to ensure that larger clusters always have multiple leaf nodes. This can be used to enhance the probability of fusing two clusters, by attempting simultaneous fusion gates between adjacent leaf nodes of the two clusters. With a probability that goes rapidly to one as the number of leaves increases, at least one of these fusion gates succeeds, fusing the two clusters together. We call this process of using leaves to fuse the two clusters with high probability *parallel fusion*.

State at the start of a round: The ideal noise-free state at the start of any round is the encoded state of the data (e.g., in the 7-qubit code), but with a number of leaves attached to each code qubit, which are used later for parallel fusion.

At the beginning of the entire trial, we assume the input is a noiseless state of this form. We justify this assumption on the grounds that the initial state does not actually matter, since our goal is to estimate the rate *per round* at which crashes occur in the encoded data. Following [19], we perform warm-up rounds of error correction before gathering data on this crash rate, so as to avoid transient effects due to the choice of initial state.

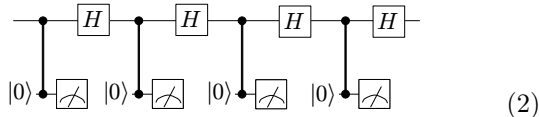
Ancilla creation: Each round of error correction involves the creation of multiple verified ancilla states, which are used to extract syndrome bits. We illustrate this for the 7-qubit code, but the procedure generalizes to other codes. We create the ancilla using the cluster:



This is a clusterization of the ancilla creation circuit in [19], with the final column of the cluster corresponding to an encoded $|+\rangle$. We abridge our notation so that touching circles represent connected cluster qubits. The cluster is created by first creating an array of microclusters; the large circles represent root nodes, while the smaller circles represent leaves; note that many of the leaves are consumed during preparation by fusion and parallel fusion, and are not shown. We then use fusion and parallel fusion to create the bonds; details appear in [15]. We conclude by measuring all qubits in the X basis, except the leaves in column 8. To verify the ancilla, we postselect on the measurement results of the terminating qubits in rows 0, 1, 2, 3 all being 0. The resulting state is an encoded $|+\rangle$, with each qubit having a number of leaves attached for the purpose of parallel fusion.

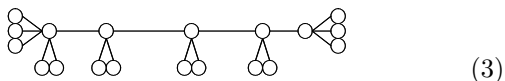
The telecorrector: To extract error syndromes we interact the data and ancillas using a special cluster state

called a *telecorrector*. Telecorrector-based syndrome extraction is a variant of Steane’s approach (c.f. also the related protocol in [20]), and can be thought of as a clustered version of the circuit:



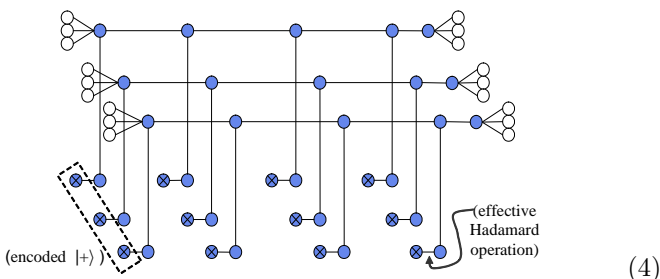
where operations are being performed on encoded qubits, $|0\rangle$ is fault-tolerant ancilla creation, and the measurement is a transversal X basis measurement.

Telecorrector creation begins with the creation of multiple copies of the following state, one copy for each qubit in the code being used:



This state can be created in the obvious way using post-selected microcluster fusion. The leaves on the left-hand end will eventually be used to attach to a single qubit of the encoded data using parallel fusion. The leaves and root node on the right-hand end will contain the output of this round of error-correction, and become the input to the next round of error-correction. The remaining leaves will be used to fuse to ancilla states.

Simultaneous with the creation of the state (3), we create four verified ancilla states, and fuse the ancillas with the leaves on the state (3) to create the state (illustrated as though for a three-qubit code):



Next we measure all the shaded qubits in the X basis, leaving only the leftmost and rightmost leaves, for later use in attaching the data, and future rounds of error correction. Applying the propagation rules for the Pauli frame, it can be shown that the measurement outcomes from the shaded qubits completely determine whether the repeated syndrome measurements will agree or not, *before the state has interacted with the data!* We have verified this fact both numerically and analytically.

We take advantage of this remarkable fact by post-selecting on measurement outcomes that ensure this *preagreeing syndrome* property. We call the resulting state the *telecorrector*. The preagreeing syndrome property enables syndrome extraction to be performed more efficiently (thus improving the threshold) than in Steane’s protocol, which extracts many syndromes to ensure that some large subset agree.

Once prepared, we use parallel fusion to attach the telecorrector to the data, and then X basis measurements to complete this part of the computation. Standard propagation rules are used to update the Pauli frame, and to determine the syndrome extracted from this procedure.

Decoding: We use a technique for syndrome decoding which takes advantage of the experimenter’s knowledge of the locations of photon loss and fusion gate failures. In particular, we use the fact (see p. 467 of [21]) that a code correcting t unlocated errors is able to correct $2t$ located errors. Our technique is a maximum likelihood procedure for decoding arbitrary combinations of located and unlocated errors. All the codes we use are CSS codes with the property that decoding of the X and Z errors can be performed separately using an identical procedure. The X -decoding procedure (for example) has the following inputs: the measured X -error syndrome, obtained from the vector of total errors of the ancilla measurement outcomes; and a list of locations (qubit indices within the code block) at which located errors have occurred during the round. The outputs of the decoding routine are: a list of locations where X flips should be made in order to correct the data; and a flag signalling a *located crash*. The located crash flag is set to “true” when different patterns of X errors are found to have equal maximum likelihood, but differ from each other by a logical X operation. The located crash flag is used to improve decoding at the next level of concatenation, by identifying encoded blocks which are known to have experienced an error.

Results of the optical cluster simulation: Our aim in simulating cluster-based error correction is to estimate the function which maps the input noise parameters (ϵ, γ) to the logical error rates, or *crash rates*, defined below. Below we describe simulations which estimate a similar function for a deterministic circuit-based protocol, and then combine the results to give the threshold curve for cluster-state optical quantum computing.

At the end of a round of simulated cluster-based error correction, we say that the round has caused a *located crash* whenever either the X or Z decoding steps have reported a located crash. We define an *unlocated crash* as follows. We take the pattern of Pauli errors on the root nodes of the data, and consider the result of a perfect (noise-free) round of correction. If perfect correction would result in a pattern on Pauli errors corresponding to a non-identity encoded Pauli operation, then we say the data has experienced an unlocated crash.

We performed simulations based on the Golay 23-qubit and Steane 7-qubit codes. For each simulation, we chose a number of settings for the noise parameters (ϵ, γ), and for each we ran a many-trial monte carlo simulation. Each trial consisted of two successive rounds of error correction, and the outcome of the trial was determined by whether the second of the two rounds caused a crash. The purpose of the first “warm-up” round is to reduce transient effects due to our choice of (noise free) initial conditions. Including more than one warm-up round did not make a statistically significant change to the results.

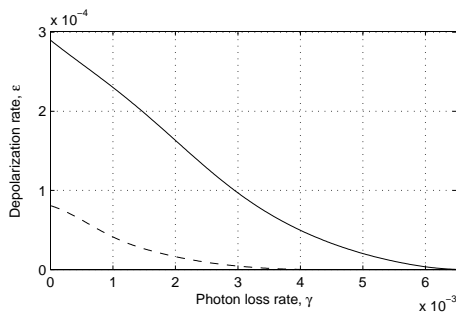


FIG. 1: Threshold region for optical clusters using the 23-qubit Golay code (solid) and 7-qubit Steane code (dashed).

We tally the outcomes as follows. For all the trials for which the first round does not cause a crash, we count: (1) the number N_U for which the second round causes an unlocated crash but not a located crash, (2) the number N_L for which the second round causes a located crash, and (3) the number N_N for which no crashes occur. The unlocated and located crash rates E and Γ are estimated as $E = \frac{N_U}{N_U + N_N}$ and $\Gamma = \frac{N_L}{N_U + N_N + N_L}$. We calculate these crash rates for a variety of input noise parameters, and use weighted least-squares fitting to fit polynomials $E(\epsilon, \gamma)$ and $\Gamma(\epsilon, \gamma)$ representing the general behaviour of the crash rates; these polynomials were in good agreement with the qualitative theory of fault-tolerance.

Concatenation: Under k layers of concatenation, our protocol is effectively equivalent to doing $k - 1$ concatenated levels of an ordinary deterministic gate-based fault-tolerance protocol, and then replacing the elements at the lowest level by cluster-based equivalents with just a single level of encoding. To understand the behaviour of

the concatenated protocol, we therefore also did simulations of a deterministic fault-tolerant protocol. These simulations followed [19], but incorporated a deterministic version of telecorrection, and the separate treatment of unlocated and located errors. The appropriate noise model has two noise parameters, (p, q) , representing, respectively, the rate of located and unlocated Pauli errors, corresponding to located and unlocated crashes at the next lowest level of concatenation. The results of our simulations suggest that these crashes may be accurately modelled as independent X and Z errors, with Y errors suppressed, and so this is the noise model we adopt. We use least squares fitting to estimate polynomials $P(p, q)$ and $Q(p, q)$, where P and Q are the rates for located and unlocated crashes at a single level of encoding in the cluster-based simulations.

Results and conclusion: Define maps $f : (\epsilon, \gamma) \rightarrow (E, \Gamma)$ and $g : (p, q) \rightarrow (P, Q)$. Then the located and unlocated crash rates after k levels of concatenation may be estimated by computing $(g^{(k-1)} \circ f)(\epsilon, \gamma)$. Provided this tends to $(0, 0)$ as $k \rightarrow \infty$ we are inside the threshold region. Fig. 1 illustrates the threshold region, and shows that the 23-qubit code gives a considerably better threshold than the 7-qubit code; resource usage will be discussed in [15]. Both codes give thresholds worse than the best known circuit thresholds [20], but the results are encouraging given the non-deterministic nature of the optical entangling operations.

Acknowledgments

Thanks to Dan Browne, Ike Chuang, Jen Dodd, Steve Flammia, and Tim Ralph for helpful discussions, and to Bryan Eastin and Steve Flammia for *Qcircuit*.

-
- [1] E. Knill, R. Laflamme, and G. J. Milburn, *Nature* **409**, 46 (2001).
 - [2] T. B. Pittman, M. J. Fitch, B. C. Jacobs, and J. D. Franson, *Phys. Rev. A* **68**, 032316 (2003).
 - [3] J. L. O'Brien, G. J. Pryde, A. G. White, T. C. Ralph, and D. Branning, *Nature* **426**, 264 (2003).
 - [4] K. Sanaka, T. Jennewein, J.-W. Pan, K. Resch, and A. Zeilinger, *Phys. Rev. Lett.* **92**, 017902 (2003).
 - [5] Z. Zhao, A.-N. Zhang, Y.-A. Chen, H. Zhang, J.-F. Du, T. Yang, and J.-W. Pan, *arXiv:quant-ph/0404129* (2004).
 - [6] M. A. Nielsen, *Phys. Rev. Lett.* **93**, 040503 (2004).
 - [7] N. Yoran and B. Reznik, *Phys. Rev. Lett.* **91**, 037903 (2003).
 - [8] R. Raussendorf and H. J. Briegel, *Phys. Rev. Lett.* **86**, 5188 (2001).
 - [9] D. E. Browne and T. Rudolph, *Phys. Rev. Lett.* **95**, 010501 (2005).
 - [10] S. Gasparoni, J.-W. Pan, P. Walther, T. Rudolph, and A. Zeilinger, *arXiv:quant-ph/0404107* (2004).
 - [11] M. A. Nielsen and C. M. Dawson, *Phys. Rev. A* **71**, 052312 (2005).
 - [12] R. Raussendorf, Ph.D. thesis, Ludwig-Maximilians Universität München (2003).
 - [13] M. S. Tame, M. Paternostro, M. S. Kim, and V. Vedral, *Phys. Rev. A* **72**, 012319 (2005).
 - [14] P. Aliferis and D. W. Leung, *arXiv:quant-ph/0503130* (2005).
 - [15] C. Dawson, H. L. Haselgrove, and M. A. Nielsen, in preparation.
 - [16] M. Varnava, D. E. Browne, and T. Rudolph, *arXiv:quant-ph/0507036* (2005).
 - [17] M. A. Nielsen, to appear in *Rev. Math. Phys.* (2005), *arXiv:quant-ph/0504097*.
 - [18] R. Raussendorf, D. E. Browne, and H. J. Briegel, *Phys. Rev. A* **68**, 022312 (2003).
 - [19] A. M. Steane, *Phys. Rev. A* **68**, 042322 (2003).
 - [20] E. Knill, *Nature* **434**, 39 (2005).
 - [21] M. A. Nielsen and I. L. Chuang, *Quantum computation and quantum information* (Cambridge University Press,

Cambridge, 2000).